



# Properties of an electroless copper process as a function of nickel and cyanide ion concentrations

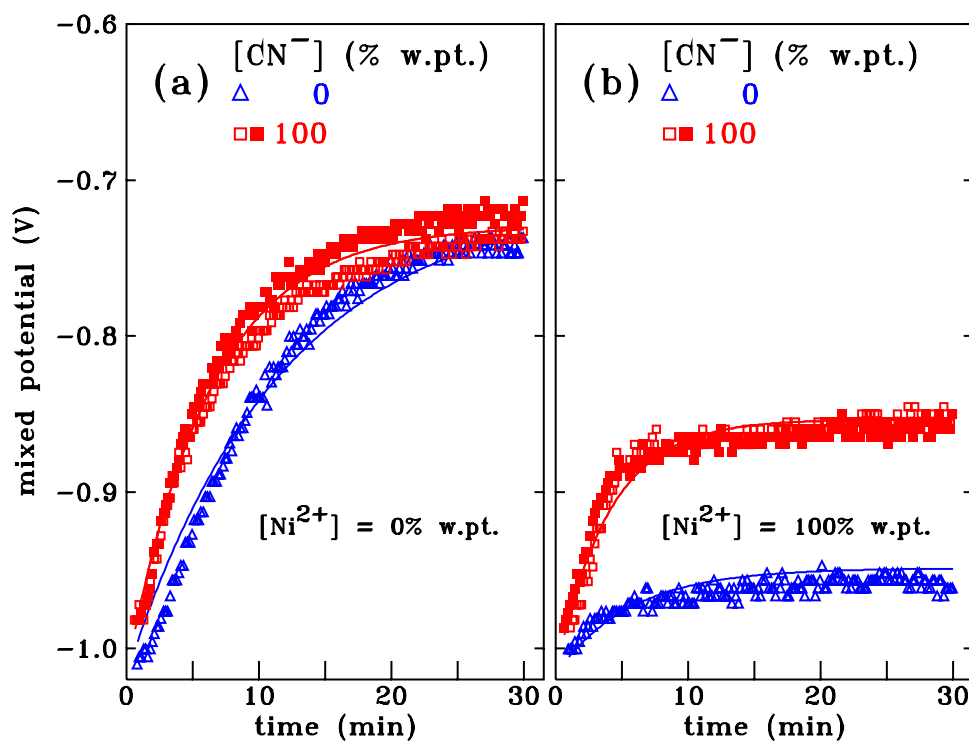
Delilah A. Brown<sup>1</sup> · Alex R. MacDonald<sup>1</sup> · Eamon A. McCarron<sup>1</sup> · Sebastian Zarwell<sup>2</sup> · Tobias Bernhard<sup>2</sup> · Ralf Brüning<sup>1</sup>

Received: 20 September 2020 / Accepted: 18 January 2021 / Published online: 14 February 2021  
© The Author(s), under exclusive licence to Springer Nature B.V. part of Springer Nature 2021

## Abstract

A cyanide-stabilized electroless copper plating process with nickel as a stress-regulating additive was investigated. Small amounts of nickel or cyanide increase the deposition rate, while large amounts of cyanide decrease the deposition rate. The steady-state mixed potential shifts by  $-0.23$  V when about 0.05 at.% nickel is co-plated with copper. Cyanide by itself does not change the mixed potential. If nickel is also present, cyanide causes an anodic shift by  $+0.09$  V. Nickel changes the stress during deposition towards tensile, while cyanide changes it towards compressive. Both nickel and cyanide accelerate the transition to steady-state plating conditions.

## Graphic Abstract



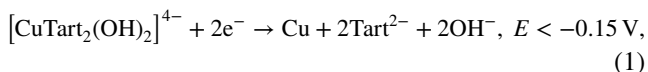
**Keywords** Electroless copper plating · Mixed potential · Plating rate · Film stress · Nickel · Cyanide

✉ Ralf Brüning  
rbruening@mta.ca

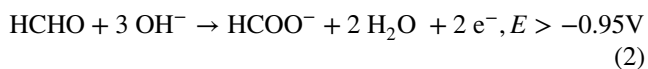
Extended author information available on the last page of the article

## 1 Introduction

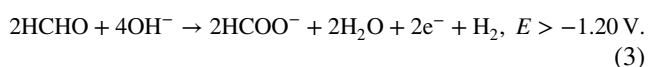
Electroless copper plating provides seed layers for galvanic plating in the production of printed circuit boards (PCBs). This study investigates the operating parameters of an electroless plating process optimized for copper-to-copper interconnections in many-layer high-density interconnect PCBs by large throughput horizontal processing. This process uses cyanide as the stabilizer [1–3], tartrate as complexant [4] and nickel to control stress during plating [5–7]. Electroless copper plating from a copper tartrate bath proceeds by



where  $E$  is the required potential of the substrate surface with respect to a standard hydrogen electrode (SHE) [8, 9]. The electrons are generated by oxidation of a reducer, formaldehyde in the present case, and transferred by the metal surface. Reactions



and



contribute about equally to the reduction of copper [7], and the potentials correspond to pH 12.7 [10].

As pointed out by Veleva, the role of cyanide in electroless plating baths is not straightforward [11]. Cyanide prevents decomposition of the metastable plating bath by sequestering  $\text{Cu}^+$  ions that can form in the solution by partial reduction of copper [2, 4]. Plating stops if its concentration is too high [12], but it may also increase the plating rate [4, 11]. Cyanide also levels the deposits by attaching itself to highly active regions of the plating surface [13, 14], and it enhances ductility [1, 15], possibly by preventing incorporation of hydrogen in the deposit [4, 7]. To assess the interaction of cyanide and nickel as bath additives, this study reports the time dependence of plating rates, mixed potential, film stress and the amount of co-plated nickel as a function of the cyanide and nickel ion concentrations in the bath as independent variables. Unlike most prior work, this study focusses on the time dependence of these parameters during the plating process.

## 2 Methods

Copper was plated in an autocatalytic process with formaldehyde as the reducer. The main components of the plating bath are shown in Table 1, with additional stabilizing

**Table 1** Bath composition and operating conditions

| Parameter   | Working point (100%) |                         | Testing range |
|---|----------------------|-------------------------|---------------|
| $[\text{Cu}^{2+}]$  | 2.25 g/L             | 0.0354 M                | –             |
| $[\text{KNaC}_4\text{H}_4\text{O}_6 \cdot 4\text{H}_2\text{O}]$ | 35 g/L               | 0.124 M                 | –             |
| $[\text{HCHO}]$   | 4.4 g/L              | 0.147 M                 | –             |
| $[\text{NaOH}]$   | 9 g/L                | 0.225 M                 | –             |
| $[\text{Ni}^{2+}]$  | 0.49 g/L             | 0.0084 M                | 0–200%        |
| $[\text{NaCN}]$   | 0.0117 g/L           | $2.39 \times 10^{-4}$ M | 0–200%        |
| Temperature   | $32 \pm 0.2$ °C      |                         | –             |
| pH  | $12.7 \pm 0.1$       |                         | –             |
| Plating time  | 15–20 min            |                         | 1–60 min      |

additives as described by References [4, 16]. The concentrations of nickel and cyanide ions were varied as indicated, and we refer to the normal operating point of the plating bath as 100%. The HCHO and NaOH concentrations were monitored via titration and adjusted to the set points as needed. The plating solutions, with a volume of 200 mL or more in a beaker, were stabilized by aeration, and during deposition, the solution was agitated with a magnetic stirrer. Freshly prepared plating solutions were conditioned by plating for 30 min.

Copper was deposited on one side of 25 mm × 25 mm × 1.5 mm glass-reinforced epoxy laminate (FR-4) substrates. The plating surface was de-smear and activated with a palladium ion solution for several minutes at 40 °C, with the back side covered with 3M 851 circuit board tape. The tape was then removed, and the palladium ions were reduced with dimethylamine borane at 30 °C to form a metallic Pd nuclei that initiate electroless copper plating. Up to eight samples were plated in the same bath for intervals ranging from 1 to 60 min. Sample masses were recorded before and after plating, and the film thickness was calculated based on the bulk density of copper. Copper film adhesion to the substrate was tested with Nichiban CT-18 rubberized cellophane tape on thirteen samples that represent the range of preparation conditions and plating times. No signs of delamination were seen upon removal of the tape. The plating potential (mixed potential) was recorded with a PASCO Xplorer GLX with respect to Ag/AgCl reference electrode with saturated KCl (Cole-Parmer RK-05990-60). For these measurements, 30 mm × 30 mm substrates were pre-plated with a 5 mm × 25 mm copper pad. Contact to this pad was made with a spring-loaded enameled copper wire with the enamel stripped at the contact points. The nickel-to-copper ratio in the films was measured with X-ray Fluorescence (XRF) with a Fischerscope XDV-SDD, and details of the analysis method have been reported previously [17]. Film stress was measured during and after plating by observing the substrate curvature of 51 μm thick Cu–Fe alloy 194 dual-leg test strips (Specialty Testing and Development Co.,

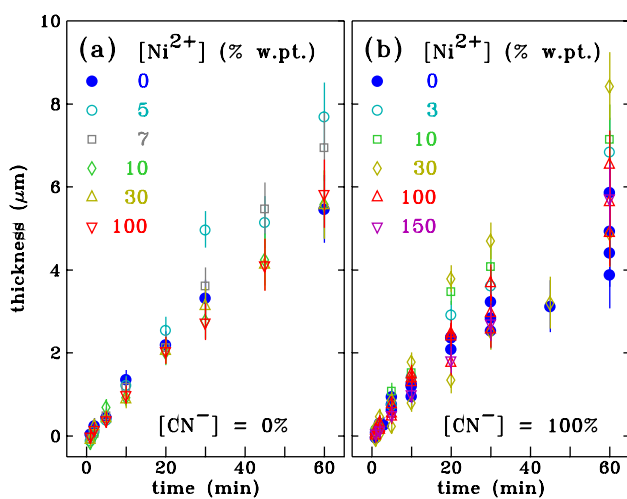
York, Pennsylvania). The two legs of the strip (7.5 cm long and 0.5 cm wide) have varnish on one side, allowing the copper to plate only on the opposite side, and deposit bends the strip in the opposite direction. Film thickness, determined via mass gain, is used along with the measured spread of the legs to calculate the stress [18]. Micrographs were obtained with a Hitachi SU3500 scanning electron microscope (SEM).

### 3 Results

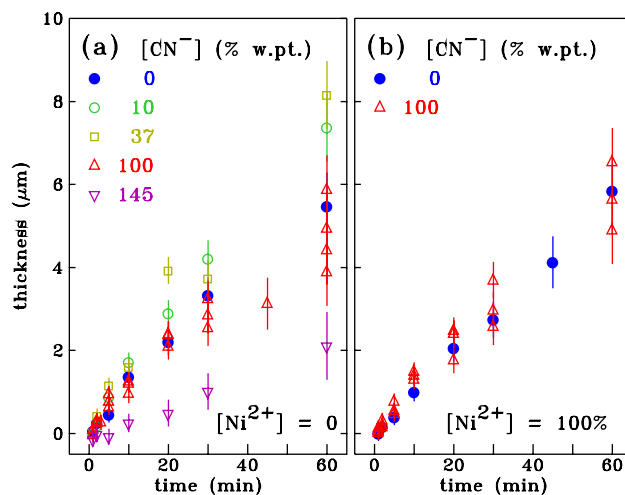
#### 3.1 Plating kinetics

Figure 1 shows the electroless deposit thickness as a function of plating time. For a stabilized bath, without nickel and cyanide (Fig. 1a), the plated thickness increases at a constant plating rate of about 0.10  $\mu\text{m}/\text{min}$ . The further data in Fig. 1a show that, in the absence of cyanide, the addition of 5 to 7% nickel speeds up plating to about 0.13  $\mu\text{m}/\text{min}$ , but it reverts back to 0.10  $\mu\text{m}/\text{min}$  at higher nickel concentrations. With 100% cyanide and without nickel, the plating rate decreases gradually with time (Fig. 1b). This indicates that the cyanide ions lead to a progressive poisoning of the plating surface. As shown by Fig. 2a, at 145% cyanide, the plating rate decreases to 0.03  $\mu\text{m}/\text{min}$  [12]. For 100% cyanide, the plating rate increases if between 3 and 100% nickel is added to the plating bath (Fig. 1b). While without cyanide, the highest plate is observed for 5% nickel, with 100% cyanide, the plating rate is highest at 30% nickel.

Figure 3 is a micrograph of a copper deposit with the nickel and cyanide concentrations at the working point. The de-smearing process prior to electroless plating creates a



**Fig. 1** Deposit thickness as a function of plating time for **a**  $[\text{CN}^-] = 0$  and **b**  $[\text{CN}^-] = 100\%$  of the working point. The nickel ion concentration was varied as indicated



**Fig. 2** Deposit thickness as a function of plating for **a**  $[\text{Ni}^{2+}] = 0$  and **b**  $[\text{Ni}^{2+}] = 100\%$  of the working point. The cyanide concentration was varied as indicated

network of pores at the surface of the FR4 substrate. These pores have a typical diameter of 10  $\mu\text{m}$ . The copper plates as a continuous layer on the walls of the pores, with nodules at the copper surface. The crystallites that form these nodules can be recognized by facets with a typical size of 0.3  $\mu\text{m}$ . Consistent plating deep within the pores indicates the high throwing power of the plating solution.

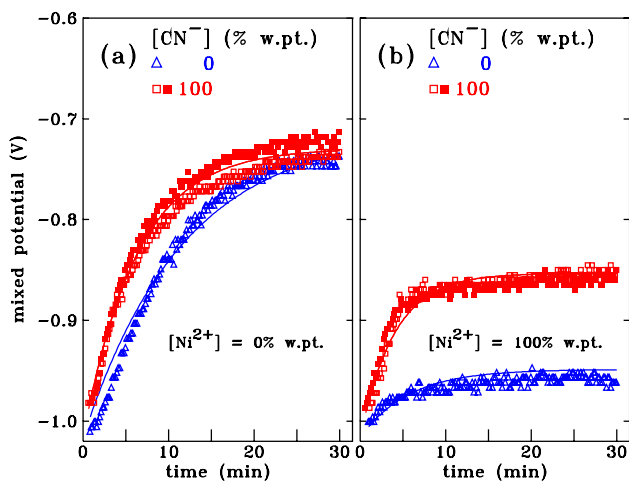
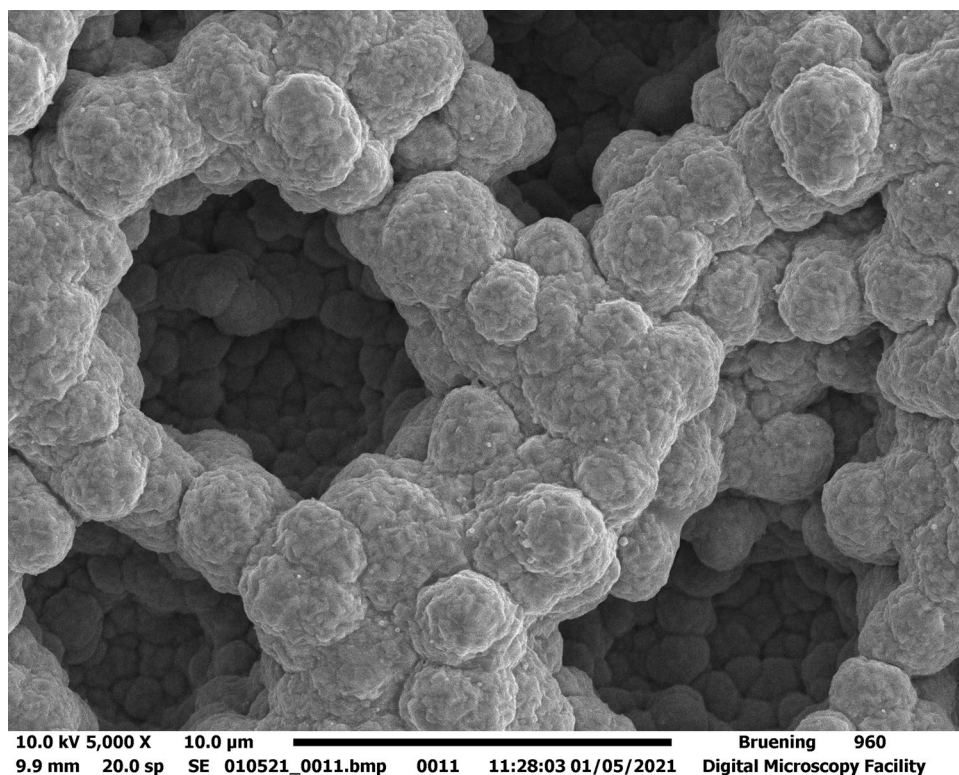
In summary, for the range  $[\text{CN}^-] \leq 100\%$ , the effects of nickel and cyanide ions on the plating rate are small. Larger amounts of cyanide reduce plating rates significantly. With both  $[\text{Ni}^{2+}]$  and  $[\text{CN}^-]$  at the working point, the plating rate is almost the same as for a solution without these ions.

#### 3.2 Mixed potential

As shown by Figs. 4 and 5, the mixed potential is  $-1.02$  V at the start of plating, measured against Ag/AgCl reference electrode, or  $-0.82$  V with respect to a SHE. This value, close to the limit for Reaction (2), reflects the high catalytic activity of the Pd nuclei and the emerging Pd–Cu alloys for the oxidation of formaldehyde [19]. The potential at the start of plating is independent of both  $[\text{CN}^-]$  and  $[\text{Ni}^{2+}]$ . Thus, we assume that the  $\text{CN}^-$  and  $\text{Ni}^{2+}$  ions in the plating solution have no direct influence on the potential, and the increase of  $E$  with time is due to cyanide ions adsorbed on the plating surface and co-plated metallic nickel.

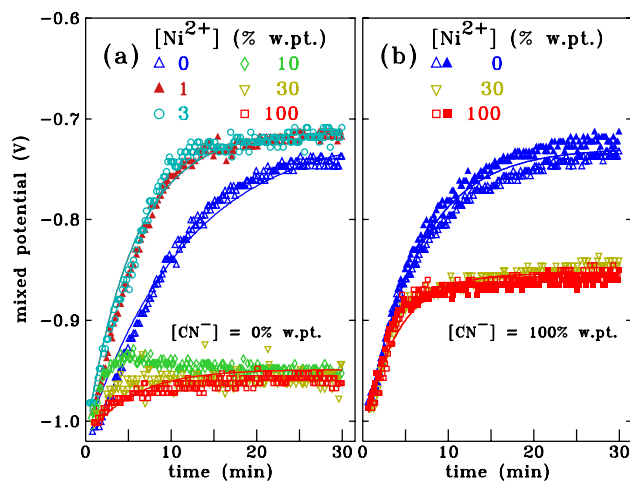
Figures 4 and 5 show that, as plating progresses, the potential increases towards steady-state values. These steady-state potentials are co-determined by the ion concentrations  $[\text{CN}^-]$  and  $[\text{Ni}^{2+}]$ . Figure 4a shows that adding  $\text{CN}^-$  ions to a Ni-free bath does not have a significant effect other than accelerating the approach to the steady state. Adding nickel to the bath strongly affects the mixed potential.

**Fig. 3** SEM micrograph of an electroless copper deposit plated on FR-4 with  $[\text{CN}^-] = 100\%$  and  $[\text{Ni}^{2+}] = 100\%$  for 20 min



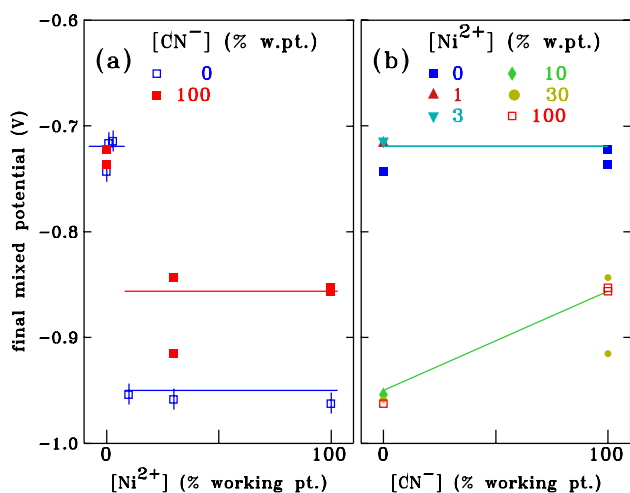
**Fig. 4** Mixed potential vs. a Ag/AgCl electrode,  $E - E_{\text{Ag/AgCl}}$ , as a function of plating time with  $[\text{CN}^-] = 0$  and 100%: **a** No nickel and **b**  $[\text{Ni}^{2+}] = 100\%$  of the working point. Solid lines are fits to the data

Figure 5a shows that the steady-state potential without nickel,  $E - E_{\text{Ag/AgCl}} \approx -0.72$  V, shifts to  $-0.95$  V upon adding 100%  $\text{Ni}^{2+}$  to the bath. This cathodic shift agrees quantitatively with the shift of the potential observed upon changing from a pure Cu substrate to a  $\text{Cu}_{90}\text{Ni}_{10}$  alloy substrate [20]. This cathodic shift requires between 3 and 10% of the working point nickel ion concentration, corresponding to  $[\text{Ni}^{2+}]/[\text{Cu}^{2+}] < 0.02$  (Table 1).



**Fig. 5** Mixed potential vs. Ag/AgCl as a function of plating time: **a**  $[\text{CN}^-] = 0$  and **b**  $[\text{CN}^-] = 100\%$  of the working point. The concentration of Ni ions was varied as indicated. Solid lines are fits to the data

Cyanide by itself has no effect on the steady-state potential (Fig. 4a), but it partially counteracts the cathodic shift of nickel by about 0.09 V (Fig. 4b). This conditional effect of cyanide suggests that it attaches to the nickel sites on the metal surface, thereby reducing their catalytic activity. Figure 6 summarizes the mixed potentials after 30 min of plating (near steady state). The two key features are (i) a cathodic shift of the mixed potential from about  $-0.72$  V



**Fig. 6** Mixed potential vs. Ag/AgCl,  $E - E_{Ag/AgCl}$  after 30 min of plating as a function of plating bath composition. **a** Data as a function of the nickel concentration. **b** The same data plotted as a function of  $[CN^-]$ . Solid lines show the steady-state potentials obtained by least-squares fits to the data

**Table 2** Parameters for the best fit of the mixed potential defined by Eqs. (4), (5) and (6)

|   |
|---|
| $E_{ss,0} - E_{Ag/AgCl} = -0.719 \pm 0.006V [-0.52V vs. SHE]$ |
| $\Delta E_{Ni,0} = -0.231 \pm 0.004V$                         |
| $\Delta E_{Ni,CN} = 0.094 \pm 0.002V$                         |
| $E(0) - E_{Ag/AgCl} = -1.016 \pm 0.002 V [-0.82V vs. SHE]$    |
| $r_0 = 0.090 \pm 0.004min^{-1}$                               |
| $r_{Ni} = 0.100 \pm 0.004min^{-1}$                            |
| $r_{CN} = 0.054 \pm 0.010min^{-1} / 100\% CN^-$               |

to  $-0.95 V$  upon adding more than 3%  $Ni^{2+}$  to the bath, and (ii) an anodic shift from about  $-0.95 V$  to about  $-0.86 V$  when cyanide ions are added to a bath that contains nickel.

The dependence of the steady-state potential on the bath composition can be summarized as

$$E_{SS} = \begin{cases} E_{SS,0} & \text{if } [Ni^{2+}] \leq 3\% \\ E_{SS,0} + \Delta E_{Ni,0} & \text{if } [Ni^{2+}] \geq 10\% \text{ and } [CN^-] = 0 \\ E_{SS,0} + \Delta E_{Ni,0} + \Delta E_{Ni,CN} & \text{if } [Ni^{2+}] \geq 10\% \text{ and } [CN^-] = 100\% \end{cases} \quad (4)$$

The numeric values, obtained by least-squares fitting, are listed in Table 2 and shown in Fig. 6. Here,  $E_{ss,0} = -0.719V$  is the steady-state mixed potential for baths with  $[Ni^{2+}] \leq 3\%$ . For baths with  $[Ni^{2+}] \geq 10\%$ , the steady-state potential undergoes a cathodic shift  $\Delta E_{Ni,0} = -0.231 V$ , and  $\Delta E_{Ni,CN} = 0.094V$  is a further anodic shift if both nickel and 100% cyanide ions are in the bath.

The time dependence of the potentials in Figs. 4 and 5 shows a transition from the value at  $t = 0$ ,  $E(0) = -1.016V$ , to the steady-state values  $E_{ss}$  given by Eq. (1). The transition follows, to a good approximation, an exponential relaxation

$$E(t) = E_{eq} + [E(0) - E_{eq}]e^{-rt} \quad (5)$$

with a rate constant  $r$  given by

$$r = \begin{cases} r_0 + [CN^-]r_{CN} \text{ if } [Ni^{2+}] = 0 \\ r_0 + [CN^-]r_{CN} + r_{Ni} \text{ if } [Ni^{2+}] \geq 1\% \end{cases} \quad (6)$$

Least-squares fits to the data with Eqs. 4, 5 and 6 are plotted in Figs. 4 and 5, and the numerical parameters are summarized in Table 2. The rate constant without nickel and cyanide is  $r_0 = 0.090min^{-1}$ . Even small amounts of nickel accelerate the rate to  $r_0 + r_{Ni} = 0.190min^{-1}$ . Cyanide also increases the transition rate to the steady state by  $0.054min^{-1}$  when  $[CN^-] = 100\%$ .

Interestingly, the curve for  $[Ni^{2+}] = 10\%$  and  $[CN^-] = 0$  in Fig. 5a shows a maximum after 5 min of plating that is not described by Eqs. 4, 5 and 6. This maximum suggests that there are two processes acting: initially the potential increases from  $E(0)$ , controlled by the catalytic activity for formaldehyde oxidation of the Cu–Pd surfaces of the palladium seeds, towards  $E_{ss,0}$ , typical for plating on a pure copper surface. However, because of co-plating of nickel in the film,  $E_{ss}$  shifts to  $E_{ss,0} + \Delta E_{Ni,0}$ , the value for Cu(Ni) films. The maximum corresponds to the instant when the rate of decrease of the catalytic activity of the disappearing Pd sites is matched by the rate of increase of the catalytic activity of the Ni sites of the Cu(Pd,Ni) alloy surface, and it appears that the nickel sites require a few minutes to become catalytically active. No maximum occurs in the mixed potential at lower nickel concentrations, where the amount of co-plated nickel is insufficient to induce the shift by  $\Delta E_{Ni,0}$ , and for nickel concentrations of 30% and higher, where the shift towards  $E_{ss,0} + \Delta E_{Ni,0}$  is more rapid.

### 3.3 Film composition

As already discussed, the plating rate and mixed potential are determined by the metallic nickel content of the plated film rather than by the amount of nickel ions in the bath. The composition of the  $Cu_{1-x}Ni_x$  films, determined by XRF, is shown in Fig. 7 as a function of the ion ratio in the plating



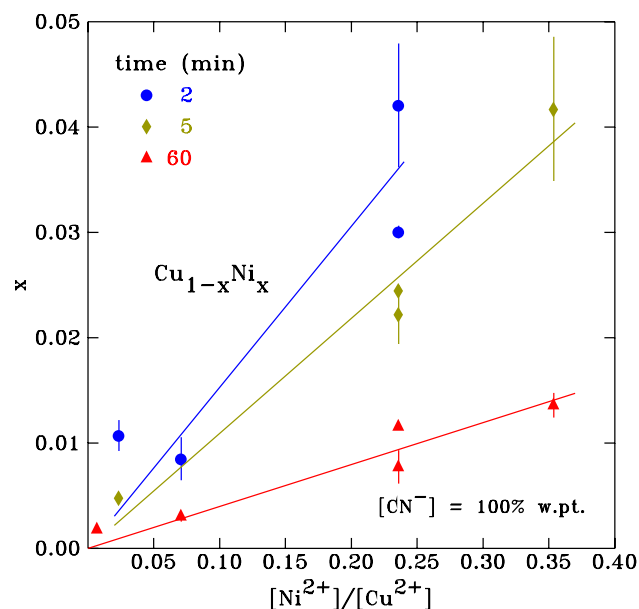


**Fig. 7** Dependence of the nickel content of the film on the ratio of nickel and copper ions in the bath at the start, during and at the end of plating. The cyanide concentration is at its working point

bath. The data show that the Ni/Cu ratio in the film is proportional to the ion ratio in the bath. The relative amount of nickel in the film decreases with plating time: at 2 min, the Ni/Cu atomic ratio in the film is about 1/6 of the ratio in the bath, and after 60 min of plating, it decreases to about 1/25, similar to previous results [7, 17]. Based on Fig. 5a, a nickel concentration between 3 and 10% of the working point is sufficient for the cathodic shift of the plating potential, corresponding to a Ni/Cu ion ratio in the bath of less than 0.023. The corresponding alloy composition is in the range from 0.03 to 0.09 at.%. Because this nickel content at the film surface is small, the catalytic activity of the nickel atom sites for Reactions 2 or 3 must be correspondingly high to drive the cathodic shift of the mixed potential.

### 3.4 Film stress

Good adhesion of the copper films requires moderate tensile (positive) film stress, since compressive stress causes blistering [21]. A significant cause of compressive stress during plating is the incorporation of hydrogen into the plated film, which can be avoided by the addition of around 100 mg/L of nickel [21]. In the present case, both the nickel and the cyanide concentration are important for the film stress. Figure 8a shows the stress-thickness product during plating with varying nickel content and the cyanide concentration kept at 100%. The stress-thickness product is proportional to the curvature of a bilayer of the Cu–Fe alloy substrate and the plated film, such that compressive/tensile stress bends the

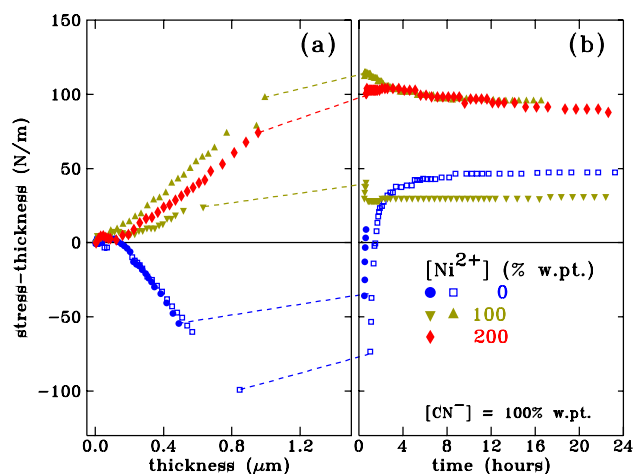


**Fig. 8** Product of film stress and film thickness for deposits with the indicated concentrations of nickel in the bath, with the cyanide concentration at the working point. The films were deposited for 30 min (closed symbols) and 60 min (open symbol). **a** Data during plating, as a function of thickness, **b** after plating, as a function of time after plating

substrate away from/towards the film side. Without nickel, stress is compressive during plating, and then switches to tensile within about 1.5 h after plating as shown by Fig. 8b. With nickel at the working point (100%) or 200%, stress during plating is tensile and remains approximately constant after plating. Plating rates on the smooth metal substrates employed here are lower than those on the rough FR4 substrates in Figs. 1 and 2.

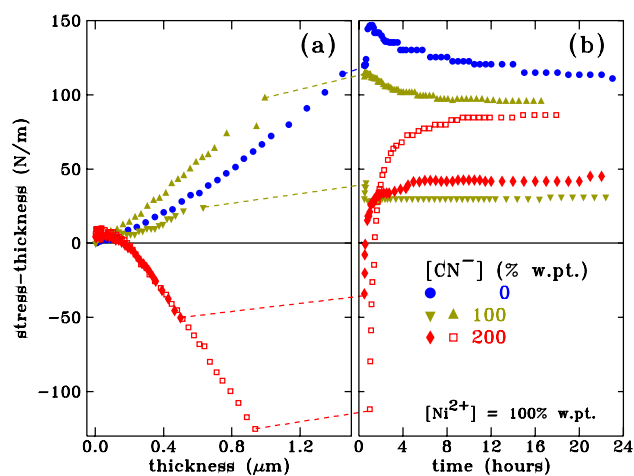


**Fig. 9** Product of film stress and film thickness for deposits with the indicated concentrations of cyanide in the bath, with the nickel concentration at the working point. The films were deposited for 30 min (closed symbols) and 60 min (open symbol). **a** Data during plating, as a function of thickness, **b** after plating, as a function of time after plating

Figure 9 shows that the effect of cyanide on the stress is opposite to that of nickel, with the stress during plating switching from tensile to compressive as cyanide is added to a bath that contains 100% Ni. If stress is compressive during plating, then it reverts to tensile after plating. With the cyanide concentration at the working point, the stress is mildly tensile, and at  $[\text{CN}^-] = 200\%$ , it is compressive. The stress of the films is summarized in Fig. 10 as a function of composition. The indicated values are the highest positive or smallest negative values during the post-deposition relaxation phase. Again, we can see that nickel increases the stress, and that cyanide decreases it.

## 4 Discussion

We have investigated the properties of a cyanide-stabilized electroless copper bath that uses tartrate as the complexant. Plating kinetics, mixed potential, film composition and deposit stress were measured as a function of the nickel and cyanide ion concentrations. Cyanide ions have the primary effect of stabilizing the bath by complexing  $\text{Cu}^+$  ions that form as an intermediate step in the reduction of copper in Reaction (1) [2]. A further effect of cyanide is to improve the ductility of the deposited copper [1, 22], attributed to adsorption of  $\text{CN}^-$  ions and thereby reducing hydrogen entrapment and embrittlement [4]. Adsorption of  $\text{CN}^-$  ions is also the likely cause for a small decrease of the plating rate seen in Fig. 2a. A further benefit of adding about 100% Ni is that it maintains the initial higher plating rate throughout the process. Nickel is also effective in accelerating deposition with other types of stabilizer systems [17]. In the case of organic additives with high affinity to the plating surface,

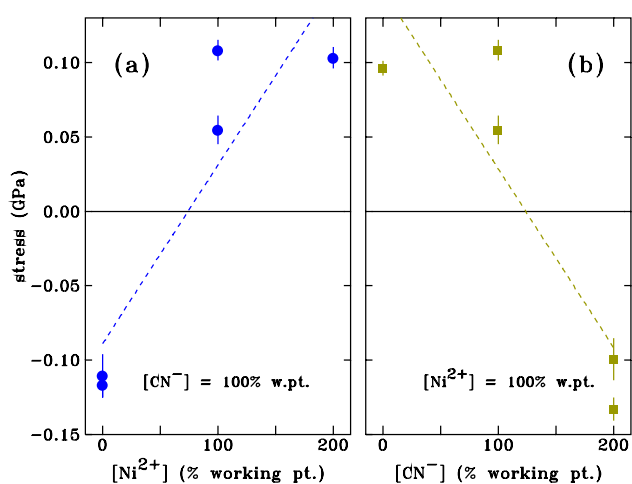


**Fig. 10** Largest stress of films during relaxation (maximum/minimum depending on sign): **a** varying nickel concentrations and cyanide at working point and **b** varying cyanide concentration with nickel at working point. Dashed lines are linear fits to the data

plating can stall completely if nickel is not added to the bath [17].

The strongest effects of nickel are a cathodic shift of the steady-state mixed potential by 0.23 V, even for small amounts ( $> 49$  mg/L), and a stress change towards tensile of about 0.18 GPa upon adding 0.49 g/L. The ability of nickel to suppress compressive stress has been reported previously [5–7]. The addition of 100% (0.0117 g/L) cyanide counteracts the nickel-induced shift of the mixed potential by +0.09 V, and for 200% the stress reverts to compressive. This raises the question about the directness of the link between the electrochemical and stress effects of nickel and cyanide. Co-deposited nickel prevents incorporation of the hydrogen generated by Reaction (2b) into the deposit, either by catalyzing hydrogen oxidation  $\text{H}_{ads} + \text{OH}^- \rightarrow \text{H}_2\text{O} + \text{e}^-$  [10, 23] or by catalyzing desorption by  $2\text{H}_{ads} \rightarrow \text{H}_2$ , thereby preventing compressive stress during plating [7]. Co-alloyed nickel also shifts the steady-state potential by catalyzing the oxidation of formaldehyde [6, 20]. As to the opposing effect of cyanide,  $\text{CN}^-$  ions may adsorb preferentially to the nickel sites of the Cu(Ni) surface, disrupting their catalytic activity. This assumption is supported by the observation that the effect of cyanide on the mixed potential is conditional on the presence of nickel. Similarly, when plating on coarse-grained copper substrates, nodular shapes appear at the ridges of the substrate surface at the start of plating when plating with nickel-containing electrolytes with organic stabilizers. These do not form with in this cyanide-stabilized plating bath, indicating the specific interaction of cyanide with the catalytic nickel sites [13].

When we consider the case of adding nickel ions to the cyanide-free plating bath, the steady-state mixed potential changes by  $-0.23$  V (Fig. 5a), while the plating rate changes only moderately (Fig. 1a). Thus, a significant cathodic shift of the potential does not lead to much faster reduction of copper. Similarly, the anodic shift of the plating potential when adding cyanide to a plating bath with 100% nickel (Fig. 4b) corresponds to no change in the plating rate (Fig. 2b). We conclude that, at least in the present case, the change of the mixed potential is not so much driver of the deposition, but rather an indicator of the extent by which Reactions (1), (2) and (3) limit the plating rate.

## 5 Conclusion

The role of cyanide in electroless copper plating processes is not straightforward, as already recognized by previous studies. While it stabilizes the bath against decomposition by sequestering cuprous ions, it can also accelerate plating as seen here for small concentrations. The effects of cyanide and nickel on the deposit stress during plating and the steady-state mixed potential are antagonistic. However,

small amounts of nickel and cyanide have, separately and jointly, an accelerating effect on the plating rate.

With cyanide and nickel at the working point, the bath formulation gives rise to good plating rates (0.10  $\mu\text{m}/\text{min}$ ), and the mixed potential reaches a steady state within about 6 min. The deposits with constant tensile stress (50–100 MPa) that contain about 1.0 at.% Ni. As shown by the time dependence of the mixed potential, the combination of the synergistic and antagonistic effects of nickel and cyanide creates a stable operating performance.

**Acknowledgements** We thank Mr. Stefan Schweder for carrying out XRF measurements. SEM images were prepared by Mr. James Ehrman.


**Funding** This study was funded by Atotech Deutschland GmbH.

## References

- Nakaso, K., Yamanoi, T., Okamura, Y., Tsuru (1985) *Electroless copper deposition solution*, US Patent 4548644
- Lu J, Wang M, Deng X, Yan J, Yun J, Jiao S (2019) Evaluation of  $\text{K}_3\text{Fe}(\text{CN})_6$  on deposition behavior and structure of electroless copper plating. *Electrochemistry* 87:214–219
- Ghosh S (2019) Electroless copper deposition: a critical review. *Thin Solid Films* 669:641–658
- Bindra P, White JR (1990) Fundamental aspects of electroless copper plating, Ch. 12. In: Mallory GO, Hajdu JB (eds) *Electroless plating fundamentals & applications*. William Andrew, New York, pp 289–329
- Bamberg S, Perry LK, Muir B, Abuzir A, Brüning F, Brüning R (2012) The effect of nickel on the strain evolution in chemical copper films. *Thin Solid Films* 520:6935–6941
- Li L-S, Li X-R, Zhao W-X, Ma Q, Lu X, Wang Z (2013) A Study of low temperature and low stress electroless copper plating bath. *Int J Electrochem Sci* 8:5191–5202
- Sharma T, Landry AE, Leger A, Brown DA, Bernhard T, Zarwell S, Brüning F, Brüning R (2018) Nickel dependence of hydrogen generation, hydrogen co-deposition and film stress in an electroless copper process. *Thin Solid Films* 666:76–84
- Ballesteros JC, Chainet E, Ozil P, Meas Y, Trejo G (2011) Electrodeposition of copper from non-cyanide alkaline solution containing tartrate. *Int J Electrochem Sci* 6:2632–2651
- Kochemirovsky VA, Fateev SA, Logunov LS, Tumkin II, Safonov SV (2014) Laser-induced copper deposition with weak reducing agents. *Int J Electrochem Sci* 9:644–658
- Shacham-Diamand Y, Dubin V, Angyal M (1995) Electroless copper deposition for ULSI. *Thin Solid Films* 262:93–103
- Veleva R (1986) Role of potassium ferrocyanide in electroless copper baths. *Surf Coat Technol* 29:87–93
- Schneble FW Jr, Zeblicky RJ, McCormack JF, Williamson JD (1968) *Process for stabilizing autocatalytic metal plating solutions*, US Patent 3403035
- Bittner A, Wanner M, Weil KG (1992) The role of the microstructure of copper deposits during electroless plating in formaldehyde containing alkaline baths. Comparison of fourier transform impedance spectroscopy and surface enhanced Raman spectroscopy. *Ber Bunsenges Phys Chem* 96:647–655
- Bernhard T, Zarwell S, Steinhäuser E, Kempa S, Brüning F (2019) The effect of Cu target pad roughness on the growth mode and void formation in electroless Cu films. In: *International Wafer Level Packaging Conference (IWLPC)*, San Jose, CA, USA, pp 1–7
- Nakahara S, Okinaka Y (1983) Microstructure and ductility of electroless copper deposits. *Acta Metall* 31:713–724
- Saubestre EB (1972) Stabilizing electroless copper solutions. *Plating* 59:563–566
- Logan E, Sharma T, Brüning F, Zarwell S, Steinhäuser E, Bernhard T, Chen N, Brüning R (2017) The effect of Ni on the kinetics of electroless Cu film deposition. *Thin Solid Films* 626:131–139
- Brüning R, Sibley A, Sharma T, Brown DA, Demay T, Brüning F, Bernhard T (2014) Stress of electroless copper deposits on insulating and metal substrates. *Thin Solid Films* 565:136–142
- Pötzelberger I, Mardare CC, Uiberlacker LM, Hild S, Mardare AI, Hassel AW (2017) Electrocatalysis on copper-palladium alloys for amperometric formaldehyde sensing. *RSC Adv* 7:6031–6039
- Meerakker JE, Bakker JWG (1990) On the mechanism of electroless plating. Part 3. Electroless copper alloys. *J Appl Electrochem* 20:85–90
- Bernhard T, Bamberg S, Brüning F, Brüning R, Gregoriades LJ, Sharma T, Brown D, Klaus M, Genzel Ch (2013) Analysis of stress/strain in electroless copper films. *Int Symp Microelectr* 2013:26–30
- Underkofler WL, Zucconi TD (1974) *Electroless copper plating*, US Patent 3844799
- Enyo M (1986) Electrooxidation of formaldehyde on Cu + Ni alloy electrodes in alkaline solutions. *J Electroanal Chem* 201:47–59

**Publisher's Note** Springer Nature remains neutral with regard to jurisdictional claims in published maps and institutional affiliations.

## Authors and Affiliations

Delilah A. Brown<sup>1</sup> · Alex R. MacDonald<sup>1</sup> · Eamon A. McCarron<sup>1</sup> · Sebastian Zarwell<sup>2</sup> · Tobias Bernhard<sup>2</sup> · Ralf Brüning<sup>1</sup> 

<sup>1</sup> Physics Department, Mount Allison University, Sackville, NB, Canada

<sup>2</sup> Atotech Deutschland GmbH, Erasmusstraße 20, 10553 Berlin, Germany